Ferromagnetic resonance studies of icosahedral Al-Mn-Pd-B alloys

1995 J. Phys.: Condens. Matter 7 9883

(http://iopscience.iop.org/0953-8984/7/50/021)

J. Phys.: Condens. Matter 7 (1995) 9883–9895. Printed in the UK

Ferromagnetic resonance studies of icosahedral Al–Mn–Pd–B alloys

D Bahadur†‖, C M Srivastava‡, M H Yewondwossen§ and R A Dunlap§

† Department of Metallurgical Engineering and Materials Science, Indian Institute of Technology, Powai, Bombay 400 076, India

‡ Department of Physics, Indian Institute of Technology, Powai, Bombay 400 076, India

§ Department of Physics, Dalhousie University, Halifax, Nova Scotia, Canada B3H 3J5

Received 17 July 1995

Abstract. Single-phase quasicrystalline alloys of the series $Al_{70-x}Mn_{15}Pd_{15}B_x$ ($0 \leqslant x \leqslant 10$) prepared by the melt spinning method have been shown to be of the icosahedral structure. Ferromagnetic resonance (FMR) studies have been undertaken in order to characterize the magnetic behaviour of these materials. The alloy with $x = 0$ exhibits a single resonance peak and does not exhibit spontaneous magnetic order. Alloys with $x \geqslant 1$ show the existence of two resonances due to two distinct Mn environments in the icosahedral structure. One resonance, resulting from non-magnetic Mn ions, shows FMR parameters which are temperature independent. The resonance resulting from magnetically ordered Mn ions shows an amplitude and field which is a function of temperature, and disappears above a critical temperature. FMR measurements are supplemented with x-ray diffraction, calorimetry and magnetization data. The magnetic behaviour of this alloy system is explained on the basis of Anderson's theory of moment formation and the indirect coupling of 3d moments.

1. Introduction

Since the first report of icosahedral order in the Al–Mn alloy system [1], a variety of Al-based ternary and quaternary systems possessing forbidden symmetry have been investigated. Of these, Al–Mn based icosahedral alloys have been particularly fascinating by virtue of a large variation in magnetic properties [2–6]. For a host, such as Al, the possibility of local moment formation on an impurity ion is at a maximum for impurities near the centre of the 3d transition metal series. For Mn in Al, a weak coupling between the sp and d electrons results in a marginal case for moment formation [7–8]. Therefore, with small variations in composition or the method of synthesis, large variations in moment formation capabilities have been reported for Al–Mn based systems. For example, a combination of Curie-like behaviour and Pauli paramagnetism has been reported in some systems indicating two kinds of Mn sites; the former being representative of localized behaviour, while the latter is representative of collective electron behaviour [5, 9]. The presence of two kinds of sites in such icosahedral alloys has been corroborated through several studies on the structural and electronic properties [2, 10–12].

Evidence for magnetic ordering in such icosahedral alloys has recently been reported in several systems. Some of the noteworthy systems are (a) Al–Mn–Si with high silicon content [13], (b) Al–Cu–Mn–Ge alloys [6, 12] and (c) the Al–Mn–Pd–M system where M = Sb,

‖ Present address: Department of Physics, Dalhousie University, Halifax, Nova Scotia, Canada B3H 3J5.

0953-8984/95/509883+13$19.50

Bi, Ge, Si and B [14–15]. These systems are metastable and are typically produced by *rapid solidification methods*. They generally possess small magnetic moments but show large coercivities and high Curie temperatures. Recently, Yokoyama *et al* [14] reported the synthesis, structural and magnetic characterization of $Al_{70-x}Mn_{15}Pd_{15}B_x$ icosahedral alloys. These alloys exhibited moments up to 18 emu g^{-1} in the icosahedral phase which disappear after crystallization at around 1000 K. The magnetic moment seems to increase with boron content up to 10 at.% B. Also noteworthy is the report by Shinohara *et al* [16] on $Al_{75}Pd_{15}Mn_{10}$ and $Al_{73}Pd_{15}Mn_{12}$ icosahedral alloys. While the former exhibits Pauli paramagnetic behaviour the latter shows a typical Curie–Weiss law. It is interesting that such a small change in composition could give rise to such a remarkable change in magnetic properties, varying from localized to itinerant electron behaviour.

In light of the above, an investigation of the icosahedral system $Al_{70-x}Mn_{15}Pd_{15}B_x$ with $0 \leqslant x \leqslant 10$ using the ferromagnetic resonance (FMR) technique has been undertaken. This method provides a variety of information regarding magnetic interactions, number of magnetic sites, magnetic transitions and magnetic anisotropy and supplements our previous investigations of transport phenomena in these materials [15]. Magnetization measurements, differential scanning calorimetry (DSC) and x-ray diffraction (XRD) studies are also reported.

2. Experimental methods

Alloys of the series $Al_{70-x}Mn_{15}Pd_{15}B_x$ with $0 \leqslant x \leqslant 10$ were prepared by quenching from the melt onto the surface of a single copper roller with the surface speed of 60 m s^{-1}. X-ray diffraction measurements were performed on a Siemens D-500 scanning diffractometer using Cu Kα radiation. Differential scanning calorimetry (DSC) measurements were made on a Dupont 9900 differential scanning calorimeter. Magnetization measurements were carried out on a conventional Faraday balance in applied fields of up to 4.0 kOe. Ferromagnetic resonance (FMR) spectra were recorded between 120 K and 500 K with a Varian associates EPR spectrophotometer operating in the X-band at 9.07 GHz. Samples used for FMR studies were in the form of thin foils (1 mm × 1 mm × 1 μm) and were mounted at the centre of a TE_{102} rectangular waveguide cavity. The steady magnetic field was applied both in parallel and perpendicular to the plane of the foil. The plot of dp/dH against H gave the information regarding the position and width of the resonance lines.

3. Results

X-ray diffraction results show that all the samples between $0 \leqslant x \leqslant 10$ are single-phase icosahedral alloys. Figure 1 shows a typical x-ray diffraction pattern for the alloys in this series. The quasilattice constant obtained from these patterns decreases monotonically as x is increased from 0 to 10. Figure 2 shows a DSC scan for a typical sample ($x = 2$). Generally, three thermal features are seen in the DSC of each sample. These are: (a) a very weak transition varying between 330 K and 630 K as x is varied between 1 and 10, (b) a very broad and large exothermic transition with the maximum temperature varying between 650 K and 700 K with x and (c) a large sharp exothermic transition occurring at yet higher temperatures. The first, (a), and the third, (c), transitions could be identified with the magnetic transition temperature and the crystallization transition of the icosahedral phase, respectively. The enthalpy associated with the larger peak (corresponding to the quasicrystalline to crystalline transformation) is fairly large for samples with a small boron

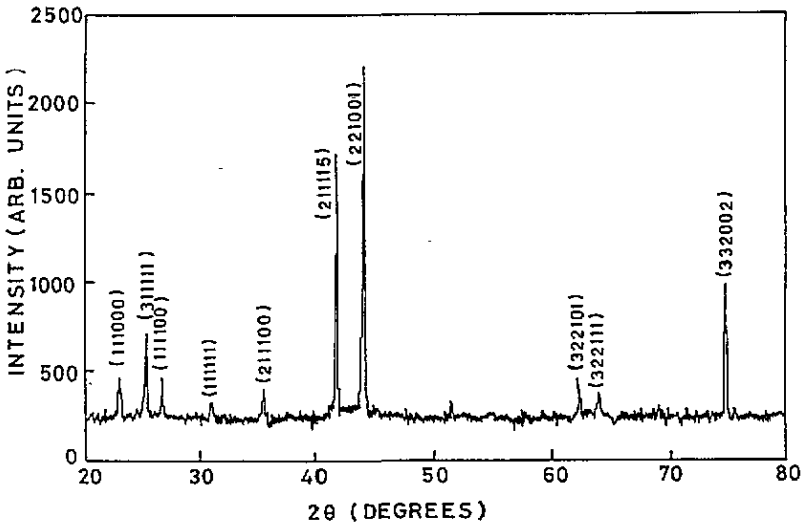

Figure 1. Room temperature Cu Kα x-ray diffraction pattern of icosahedral $Al_{68}Mn_{15}Pd_{15}B_2$.

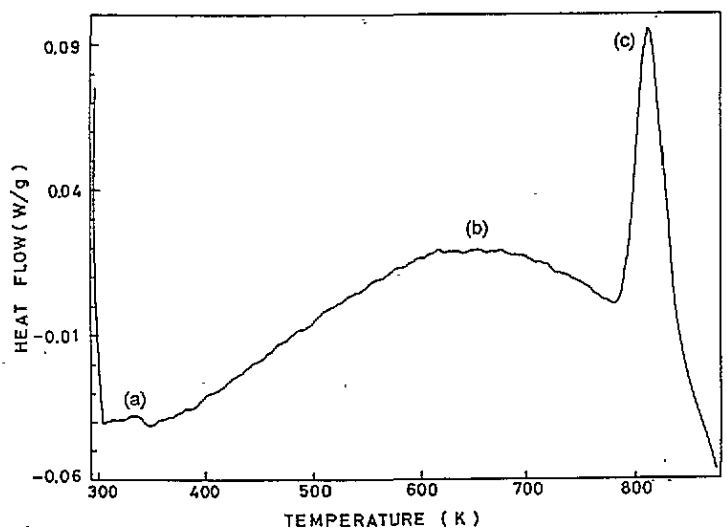

Figure 2. Differential scanning calorimetry (DSC) curve for icosahedral $Al_{68}Mn_{15}Pd_{15}B_2$.

concentration while it is much smaller for samples with higher boron concentration. Typical values of enthalpy for samples with $x = 2$ and 6 are 24.4 and 2.4 kJ kg^{-1}, respectively. The origin of the second broad transition, (b), is not so clear. However, on the basis of previous reports [12, 17] for quasicrystals, this can most likely be attributed to structural relaxation of disorder and phason strains introduced in the system during the quenching process. Recently, there has been a number of reports of such a broad transition, particularly in the samples synthesized through non-equilibrium methods [9, 12, 17].

The magnetization measurements show some interesting features. For the sample with $x = 0$, there is no indication of magnetic order. With 1 at.% boron introduced into the

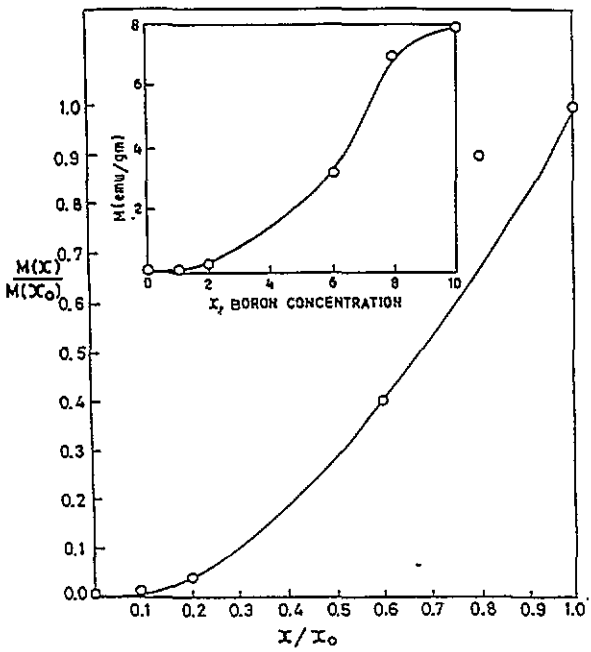

Figure 3. Reduced magnetization, $M(x)/M(x_0)$, as a function of (x/x_0) with $x_0 = 10$ measured at room temperature for icosahedral $Al_{70-x}Mn_{15}Pd_{15}B_x$. The theoretical curve is shown by the solid line. The inset shows the magnetization value at 4.2 K as a function of boron concentration.

system, a spontaneous magnetic moment is observed which increases with increasing boron concentration. Figure 3 shows $M(x)/M(x_0)$ as a function of (x/x_0) for $0 \leqslant x \leqslant 10$ with $x_0 = 10$. The inset shows the magnetization measured at a field of 4 kOe as a function of boron concentration. As the boron concentration increases, the magnetization increases for samples with x up to at least 10. A similar observation has been made by Yokoyama *et al* [14]. This indicates that the number of Mn atoms contributing to the magnetic interaction increases with boron content up to $x = x_0$. In figure 4 the magnetization is shown as a function of applied magnetic field for samples with $x = 8$ and 10. These data do not show evidence of saturation up to a field of 4 kOe. Also, the magnetization measurements show some hysteresis with a sizable remanance indicating the hard magnetic character of these materials. The unusual magnetic properties are somewhat similar to the weak ferromagnetic behaviour of disordered Ni_3Mn which shows field-dependent magnetization that does not saturate at 4 K [18]. Among Al–Mn-based quasicrystals, such behaviour is often observed [12, 13].

Ferromagnetic resonance studies have been carried out (both in parallel and perpendicular configurations) as a function of temperature and composition. Typical FMR spectra obtained at 173 K for the icosahedral system $Al_{70-x}Mn_{15}Pd_{15}B_x$ with $0 \leqslant x \leqslant 10$ are illustrated in figure 5. Figure 6 shows FMR spectra for both the parallel and perpendicular configurations for the alloy with composition with $x = 8$ at temperatures of 273 and 298 K. In figures 7(a) and (b), typical FMR spectra for alloys with compositions $x = 2$ and 10, respectively, are illustrated for different temperatures. A comparison of figures 5 through to 7, which are typical of all the FMR results for all samples studied here, allows for the following important conclusions.

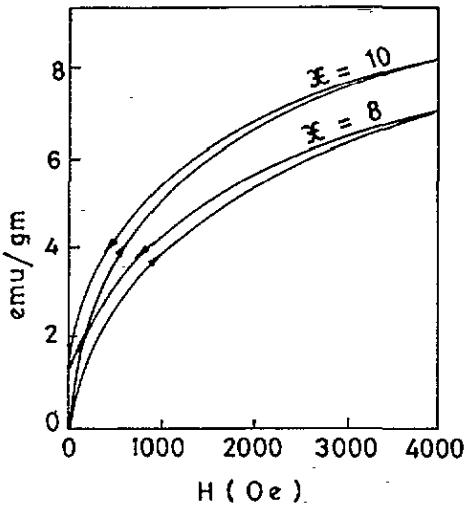

Figure 4. Room temperature magnetization as a function of applied magnetic field for icosahedral $Al_{70-x}Mn_{15}Pd_{15}B_x$ ($x = 8$, 10) showing hysteresis.

(a) As seen in figure 5, there are two lines for $0 < x \leqslant 10$ for which the first resonance field $H_r \approx 3000$ Oe, while for the other $H_r \ll 3000$ Oe. The position and the intensity of the low-field line is a sensitive function of the temperature and it disappears above a certain temperature which is considered to be the critical temperature T_c of the sample. Also, for $x = 0$, only a single resonance is observed at a field of 3040 Oe for temperatures above 77 K. For $x = 2$, as shown in figure 7(a), where the spectra are plotted for various values of the temperature, the low-field line disappears at $T_c \approx 350$ K similar to that reported by Misra *et al* in case of Al–Mn–Si alloys [19]. Table 1 gives the values of T_c determined in this way for different values of x. The transition temperatures estimated from DSC measurements for these samples are also given in the table.

Table 1. Transition temperatures estimated from FMR and DSC data for icosahedral $Al_{70-x}Mn_{15}Pd_{15}B_x$ ($0 \leqslant x \leqslant 10$).

x	T_c from FMR (K)	T_c from DCS (K)
1	320	325
2	350	340
6	410	415
8	450	470
10	500	490

(b) All the spectra are taken at 9.07 GHz and the DPPH line is at 3240 Oe. The line close to 3000 Oe which is present for all values of x and T has a free spin g-value close to 2. From figure 5, it is seen that the intensity of this line varies with x and for the larger values of x it tends to decrease. It is also observed that the intensity of this increases significantly when the boron concentration is increased from $x = 0$ to $x = 1$. On further increase of x, the low-field line grows at the expense of the high-field line. This may be accounted for by assumuing that at $x = 0$, most of the spins are in an itinerant state and these become localized as soon as boron is introduced. With the increase in x, the pair

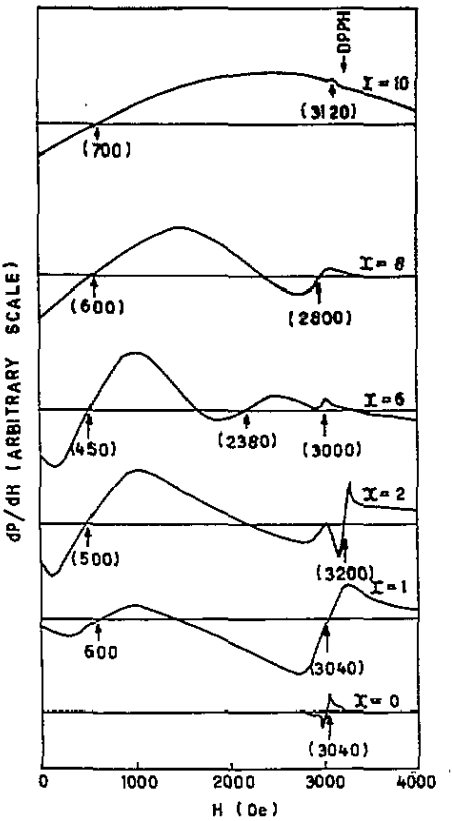

Figure 5. Ferromagnetic resonance (FMR) spectra recorded in the perpendicular configuration at 173 K for icosahedral $Al_{70-x}Mn_{15}Pd_{15}B_x$ ($0 \leqslant x \leqslant 10$).

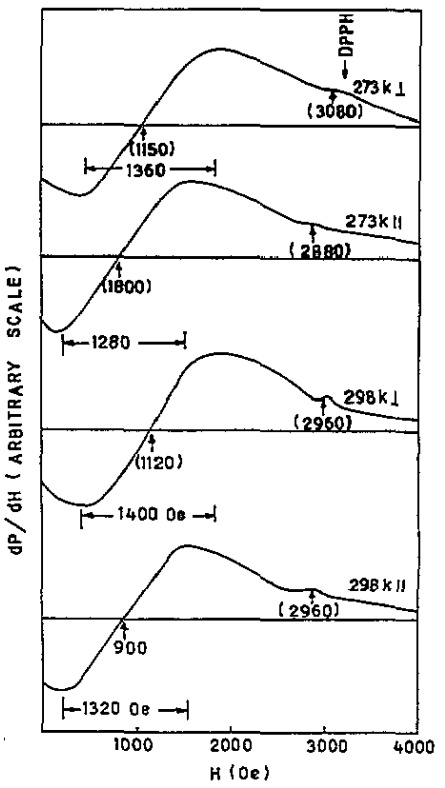

Figure 6. FMR spectra recorded in parallel (||) and perpendicular (⊥) configurations for icosahedral $Al_{62}Mn_{15}Pd_{15}B_8$ at 273 K and 298 K.

interaction presumably grows and the low-field line begins to dominate.

(c) In figure 6, the resonance field $H_\perp$ is larger than $H_\parallel$ in each case. The difference, $H_\perp - H_\parallel$, as shown later is proportional to $4\pi M$. As x is increased, the difference increases, reaches a maximum of 200 Oe and decreases again for $x = 10$. These differences for samples with $x = 8$ and 10 are illustrated in figure 8.

(d) As shown in figures 7(a) and (b), the low-field line is highly asymmetric. With increasing temperature, its intensity is observed to decrease and its line position shifts to higher fields. The high-field line with $g \approx 2$ is essentially independent of temperature in the range 130 to 500 K. It is shown later that the shift of the low-field line is due to the presence of the anisotropy field.

The FMR lineshapes shown in figures 7(a) and (b) are highly asymmetric. Spano and Bhagat [20] have made a detailed study of ferromagnetic resonance in amorphous transition metal–metalloid alloys. They have concluded that the experimental lineshapes are not reproducible and the frequency dependence of linewidths indicates that the amorphous materials are magnetically inhomogeneous regardless of spin concentration. This would be equally applicable to the present icosahedral compounds, particularly since the magnetic

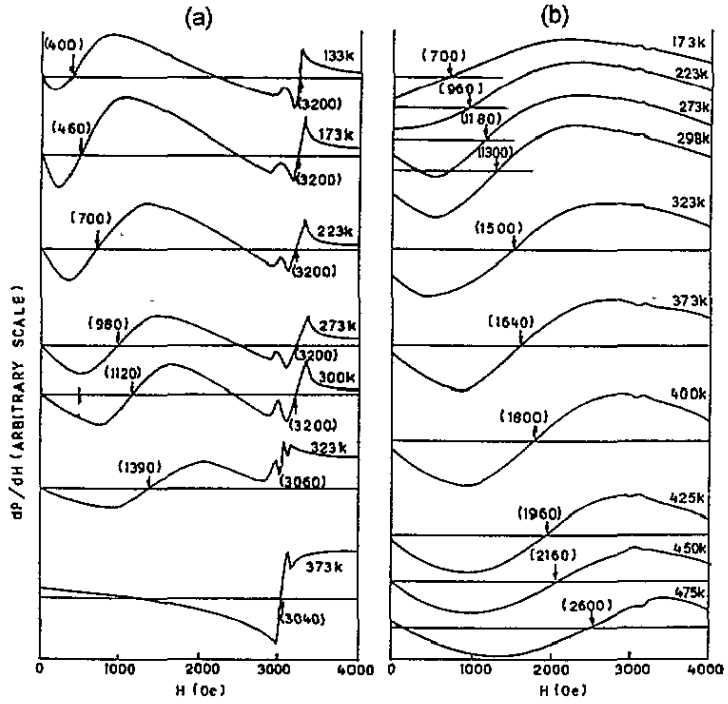

Figure 7. FMR spectra recorded in the perpendicular configuration at different temperatures for icosahedral (a) $Al_{68}Mn_{15}Pd_{15}B_2$ and (b) $Al_{60}Mn_{15}Pd_{15}B_{10}$.

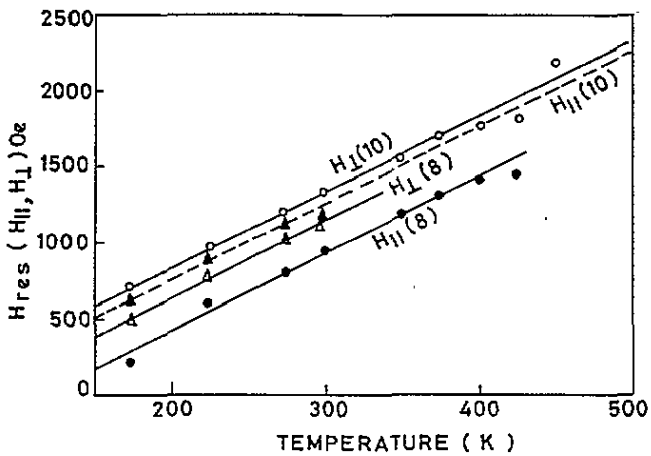

Figure 8. Resonant field (for the first resonance) for parallel (∥) and perpendicular (⊥) configurations as a function of temperature for icosahedral $Al_{70-x}Mn_{15}Pd_{15}B_x$ ($x = 8$, 10).

component is only 15%. Since the magnetization is field dependent, the line width is observed to be dependent on the field.

An anisotropy field, H_{an}, may be included in Kittel's equation. For the parallel and

perpendicular resonance, this gives the resonance fields as [21,22]:

$$\left(\frac{\omega}{\gamma}\right)^2 = (H_\parallel + H_{an})(H_\parallel + H_{an} + 4\pi M) \tag{1}$$

$$\left(\frac{\omega}{\gamma}\right) = (H_\perp + H_{an} - 4\pi M) \tag{2}$$

where ω is the angular microwave frequency and γ is the gyromagnetic ratio. As discussed by Jackson *et al* [22] for amorphous TM–metalloid systems, H_{an} is not the magnetocrystalline anisotropy field and the applied field direction is the easy direction in every case. This is observed in the present icosahedral system also. In the present case, $H_{an} \approx 3000$ Oe and $4\pi M \approx 100$ G and it can easily be shown that

$$H_\perp - H_\parallel \approx \tfrac{3}{2}(4\pi M). \tag{3}$$

Since the sample is unsaturated, $4\pi M$ denotes the magnetization at the mean field $\frac{1}{2}(H_\perp + H_\parallel)$. From the high-field resonance, the g-value for $x = 10$ is found from figure 7(b) to be 2.14 and is independent of temperature between 133 and 475 K. It is assumed that the low-field resonance line also has the same g_{eff}-value. From figure 5, the g_{eff}-values were obtained for different values of x at 173 K and are given in table 2. It appears that there is no simple systematic dependence of g_{eff} on boron concentration, x. However, as seen from figure 7, for a given value of x, g_{eff} is independent of temperature.

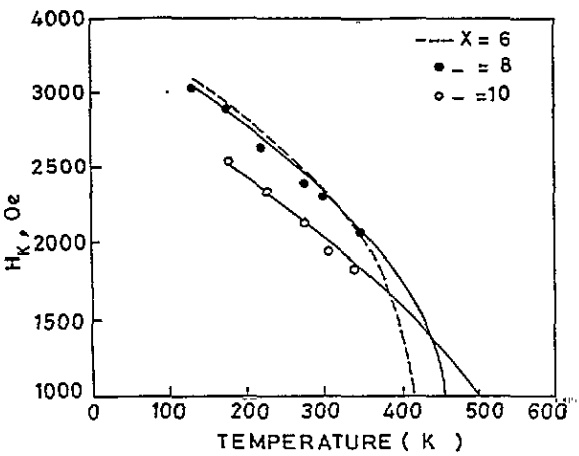

Figure 9. Variation of the anisotropy field as a function of temperature for icosahedral $Al_{70-x}Mn_{15}Pd_{15}B_x$ ($x = 6$, 8, 10).

Table 2. Values of g_{eff} obtained for different values of x at 173 K.

x	0	1	2	6	8	10
g_{eff}	2.13	2.13	2.02	2.16	2.23	2.14

For different values of x and T, values of H_{an} are obtained using equation (2), ω/γ is given by $\nu = 9.07$ GHz and g_{eff} is given above. The values of H_{an} so obtained are

plotted in figure 9 as a function of temperature for some typical values of x. The lineshape in figure 7(b) is approximately given by a Lorentzian function

$$\frac{dp}{dH} = \frac{A(H - H_0)\Delta H}{[(H - H_0)^2 + \Delta H^2]^2} \tag{4}$$

where H_0 is the resonance field, A is a constant for a given temperature and the apparent linewidth ΔH has a constant value of large magnitude of the order of the anisotropy field. In figure 10, equation (4) is plotted for two temperatures, 173 and 298 K, for $x = 10$ with the parameters given in table 3. The experimental values agree well over most of the resonance except at high fields. This deviation may be due to the incomplete saturation of the sample. This is clear from the magnetization curve given in figure 4 where it is seen that the sample is not saturated in the resonance region. The $4\pi M$ value which is obtained from equation (3) is the value of the magnetization at $\frac{1}{2}(H_\perp + H_\parallel)$. It is worthwhile examining whether the values obtained through the resonance data agree with the magnetization data. Since the magnetization measurements are taken at room temperature, the resonance fields $H_\perp$ and $H_\parallel$ for $x = 8$ at $T = 298$ K are considered. These data give $4\pi M = \frac{2}{3}(1150 - 910) = 160$ G. On the other hand, from figure 4, for the field $\frac{1}{2}(1150 + 910) = 1030$ Oe, a value of $M = 3.85$ emu g^{-1} is obtained for $x = 8$. The density of this alloy is 4.78 g cm^{-3} and this gives $4\pi M = 231$ G. In view of the uncertainty of Kittel's equation describing the resonance condition for the unsaturated samples, this agreement is not unsatisfactory. In fact, this agreement is poorer for $x = 10$ for which $4\pi M$ at 298 K is found to be 80 G by resonance and 330 G by the magnetization measurements.

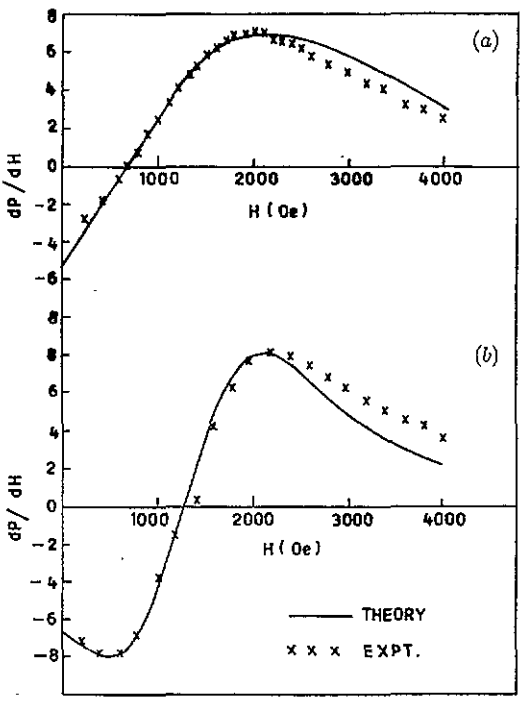

Figure 10. Plot of dp/dH versus field at (*a*) 173 and (*b*) 298 K for icosahedral $Al_{70-x}Mn_{15}Pd_{15}B_x$ ($x = 10$).

Table 3. Parameters for equation (4) as plotted in figure 10 at temperatures of 173 and 298 K for $x = 10$.

T (K)	173	298
H_0 (Oe)	700	1300
A ($\times 10^{-7}$)	12.12	4.87
ΔH (Oe)	2390	1400

These results indicate that due to variation of exchange and anisotropy energies arising from the random distribution of Mn ions, non-saturation of magnetization occurs. Unlike the ferromagnetic case, the spins are non-collinear and it is difficult to achieve saturation. This may also account for inhomogeneous broadening of the lines. A detailed analysis is not possible due to uncertainties in the site occupation of Mn ions as well as the existence of Mn–B–Mn configurations. The discussion in the following section may account for the magnetic coupling between the pairs of Mn atoms.

4. Discussion

In the context of the results presented above, the following conclusions may be drawn.

The Mn atoms exist in two magnetic states when boron is introduced into the icosahedral alloy, $Al_{70}Mn_{15}Pd_{15}$. These states are as free Mn ions in the paramagnetic state and as pairs of magnetically coupled Mn–Mn ions which experience a large local anisotropy field whose origin is not yet understood. This type of anisotropy field, whose easy direction always coincides with the external field, has been observed in amorphous alloys and is very different from magnetocrystalline anisotropy energy. As the concentration of boron atoms is increased, the pair interaction of the Mn–B–Mn configuration leads to spontaneous magnetization which is proportional to the square of the boron concentration. The random distribution of such magnetically coupled pairs within the icosahedral structure results in a large distribution of exchange energies leading, not only to the magnitude, but also to sign variation of these interactions among the magnetically coupled pairs. This leads to the dependence of the magnetization on the field even at very large fields and hence to incomplete saturation. The present results show that the ferromagnetic resonance lineshape for the partially magnetized system can still be adequately described as a Lorentzian. The applicability of Kittel's resonance condition, in this case, is questionable since the roles of the demagnetizing and the anisotropy fields in the partially magnetized systems can not be properly analysed.

A simple model for the magnetic coupling of Mn atoms through boron may now be proposed. Considering the fact that without boron the sample does not exhibit any magnetic order and that even 1 at.% of boron induces magnetic interaction, it is unlikely that the magnetic ordering of the Mn atoms originates from the RKKY interaction. On the basis of the electronic configuration of boron ($2s^2 2p^1$) compared with that of aluminum ($3s^2 3p^1$) or on the basis of the change in the measured lattice parameter it would be difficult to justify the importance of the RKKY interaction in this system. Yokoyama *et al* [14] have also concluded that the RKKY interaction is unlikely and suggest that the origin of magnetic interaction appears complicated. The dependence of the magnetic properties (i.e. the spontaneous magnetization and transition temperature) on the concentration of boron suggests local moment formation as is prevalent in many Mn-containing icosahedral alloys. Since the tendency for local magnetic moment formation on an impurity ion in an Al host

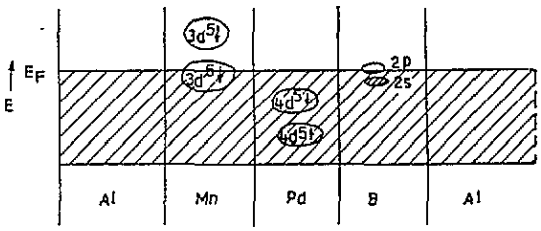

Figure 11. Proposed model of virtual bound levels of magnetic impurities Mn and Pd and non-magnetic impurity B in icosahedral $Al_{70-x}Mn_{15}Pd_{15}B_x$ with aluminum providing the conduction band states of the matrix.

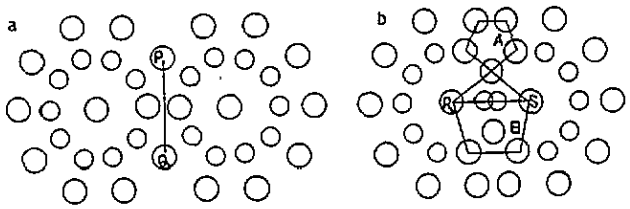

Figure 12. Structural model showing two types of edge-sharing icosahedra (adapted from [24]).

alloy is maximum for Mn [7, 8], the magnetic order in the present alloys presumably arises as a result of local Mn moment formation. As the magnetic behaviour is found to be strongly dependent on the boron concentration, it is likely that the boron sp electrons contribute to the magnetic interactions between the 3d electrons of neighbouring Mn atoms.

In the quasicrystal $Al_{70-x}Mn_{15}Pd_{15}B_x$, B may be treated as a non-magnetic impurity and Mn and Pd as magnetic impurities in the Al matrix. As discussed by Anderson [23], there is a splitting of the d shell of the transition metal atom in an sp matrix of a metal like Al or Cu into two virtual bound levels of opposite spin direction as a result of the s–d interaction. The s and p levels of boron in aluminum can be assumed to behave as virtual bound states located close to the Fermi level, E_F, as illustrated in figure 11. The position of these levels with respect to E_F depends on the site that the B atom occupies in the icosahedral structure and the nature of its nearest neighbours.

Following Higara *et al* [24] the quasicrystalline structure may be modelled using a fundamental icosahedral unit of edge length of a_0 which consists of a central Mn atom and twelve surrounding atoms, which, in the present case, are $9 - x/7.5$ Al, 1 Mn, 2 Pd and $x/7.5$ B atoms. A larger icosahedron with an edge length of a_l is constructed by aggregating twelve a_0 icosahedra. This structure is illustrated in figure 12.

On the basis of this model, the possibility of magnetic interactions between the central Mn atoms of neighbouring icosahedra may be examined. Since the distance between Mn atoms is large, direct overlap of wave functions is not possible. The coupling between the spins at neighbouring Mn sites is, therefore, expected to arise from an indirect exchange interaction. As discussed previously, the RKKY mechanism does not seem to agree with experiment. Since, with only a small addition of boron, magnetic ordering occurs, it is expected that the p orbital of boron plays a major role in the magnetic interactions. In figure 13, the two boron atoms located closest to the Mn–Mn bond axis in the RS and PQ edge-sharing configurations of figure 12 are illustrated. These atoms have their p orbitals oriented in the π-bonding configuration for maximum overlap with the d orbitals. It is obvious that magnetic coupling can occur only in the RS configuration. The $2p_\pi$ virtual bound molecular states of B^{2-} in this configuration may play the same role as the 2p states

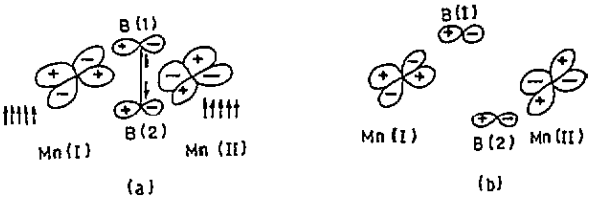

Figure 13. Arrangement of Mn and B atoms in (a) RS and (b) PQ edge-sharing icosahedral configurations as shown in figure 12. Only Mn atoms in RS configurations are magnetically coupled.

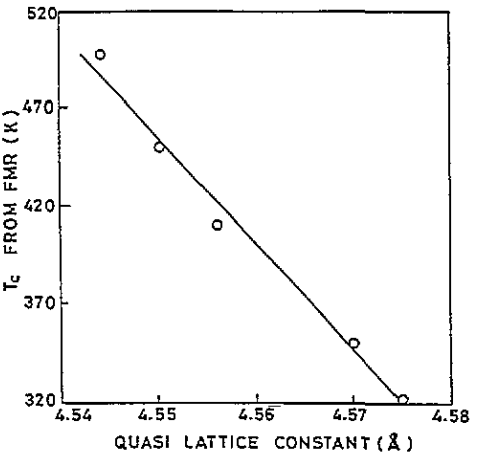

Figure 14. Transition temperature as estimated from FMR spectra as a function of quasilattice constant for icosahedral $Al_{70-x}Mn_{15}Pd_{15}B_x$ ($0 \leqslant x \leqslant 10$).

of O^{2-} for the superexchange interaction in MnO. An electron with minus spin is transferred from p_π to Mn(I) which is assumed to have five spins oriented in the plus direction. The remaining spin in the doubly degenerate p_π orbital is also pointing down and can lower its energy through exchange with the spins of the 3d subshell on Mn (II). If this exchange has a negative sign, the spin of Mn(II) should be pointing up. Consequently, spins on Mn(I) and Mn(II) are coupled ferromagnetically. As the concentration of boron atoms increases, its p state will acquire a more itinerant character and will cease to provide magnetic coupling between Mn atoms. On the basis of this model it is expected that beyond a certain value of x in $Al_{70-x}Mn_{15}Pd_{15}B_x$ the magnetic properties would begin to diminish.

It is also possible to estimate the Mn magnetic moment as a function of the boron concentration. The magnetic coupling between Mn atoms in the above model should be proportional to the probability of the simultaneous occupation by boron atoms of sites 1 and 2 surrounding the two nearest neighbours located at the RS edge-sharing icosahedra. Since this probability is proportional to x^2, it is expected that for small values of x, $M(x)$ should vary as x^2. As discussed above, this relation should hold only up to some value of x, beyond which it should either remain constant or decrease. Figure 3 shows $M(x)/M(x_0)$ as a function of x/x_0 where x_0 is taken to be $x_0 = 10$ for the $Al_{70-x}Mn_{15}Pd_{15}B_x$ series. The solid line in the figure is the theoretical curve $M(x)/M(x_0) = (x/x_0)^2$. The agreement with the experimental points is seen to be satisfactory.

The relationship of the Curie temperature, T_c, and the quasilattice constant, a_0, as illustrated in figure 14, shows that as the boron concentration, x, is increased, a_0 decreases

and T_c increases due to larger overlap of the wave functions. Such a linear dependence of T_c is often observed in ferrimagnetic systems [25] where it is widely believed that the superexchange mechanism is responsible for the spin ordering.

5. Conclusions

Ferromagnetic resonance studies of icosahedral quasicrystals in the melt-quenched Al–Mn–Pd–B alloy system have indicated that local magnetic moments form on some Mn sites and are coupled through boron atoms when neighbouring icosahedra are in a specific edge-sharing configuration. The uncoupled Mn atoms behave as paramagnetic ions and give a temperature-independent resonance peak with a free spin g-factor. Coupled spins give a strongly temperature-dependent resonance whose intensity decreases with increasing temperature and vanishes at the Curie temperature. The magnetic behaviour of this alloy system has been explained on the basis of Anderson's theory of moment formation and indirect coupling of 3d moments through the induced polarization of the intervening p shells.

Acknowledgments

This work was funded by the Department of Science and Technology, Government of India and the Natural Sciences and Engineering Research Council of Canada.

References

[1] Shechtman D, Blech I, Gratias D and Cahn J W 1984 *Phys. Rev. Lett.* **53** 1951
[2] McHenry M E, Srinivas V, Bahadur D, O'Handley R C, Lloyd D J and Dunlap R A 1989 *Phys. Rev.* B **39** 3611
[3] Eibschutz M, Chen H S and Hauser J J 1986 *Phys. Rev. Lett.* **56** 169
[4] Bellisent R, Hippert F, Monod P and Vigneron F 1987 *Phys. Rev.* B **36** 5540
[5] Srinivas V, McHenry M E and Dunlap R A 1989 *Phys. Rev.* B 40 9590
[6] Tsai A P, Inoue A, Masumoto T and Kataoka N 1988 *Japan. J. Appl. Phys.* **27** L2252
[7] Eibschutz M, Lines M E, Chen H S, Waszczak J V, Espinosa G P and Cooper A S 1990 *Phys. Rev.* B **41** 4606
[8] Moruzzi V L, Marcus P M and Pattnaik P C 1988 *Phys. Rev.* B **37** 8003
[9] Bahadur D and Singh K 1993 *J. Magn. Magn. Mater.* **119** 76
[10] Bahadur D, Gaskell P H and Imeson D I 1987 *Phys. Lett.* **120A** 417
[11] Eibschitz M, Lines M E, Chen H S, Waszczak J V, Papaefthymiou G and Frankel R B 1987 *Phys. Rev. Lett.* **59** 2443
[12] Bahadur D, Singh K and Roy M 1992 *Mater. Sci. Eng.* A **154** 79
[13] Dunlap R A, McHenry M E, Srinivas V, Bahadur D and O'Handley R C 1989 *Phys. Rev.* B **39** 4808
[14] Yokoyama Y, Inoue A and Masumoto T 1992 *Mater. Trans. JIM* **33** 1012
[15] Yewondwossen M H, Ritcey S P, Yang Z and Dunlap R A 1994 *J. Appl. Phys.* **76** 6499
[16] Shinohara T, Yokoyama Y, Sato M, Inoue A and Masumoto T 1994 unpublished
[17] Eckert J, Schultz L and Urban K 1990 *Z. Metalk.* **81** 862
[18] Kouvel J 1958 *J. Appl. Phys.* **29** 518
[19] Misra S K, Misiak L E, Bahadur D, Srinivas V and Dunlap R A 1989 *Phys. Rev.* B **40** 7537
[20] Spano M L and Bhagat S M 1981 *J. Magn. Magn. Mater.* **24** 143
[21] Webb D J and Bhagat S M 1984 *J. Magn. Magn. Mater.* **42** 109
[22] Jackson E M, Liao S B, Bhagat S M and Manheimer M A 1989 *J. Magn. Magn. Mater.* **80** 229
[23] Anderson P W 1962 *Phys. Rev.* **124** 541
[24] Hiraga K, Hirabayashi M, Inoue A and Masumoto T 1985 *Sci. Rep. Res. Inst. Tohoku Univ.* A **32** 3090
[25] Smit J and Wijn H P J 1959 *Ferrites: Physical Properties of Ferrimagnetic Oxides in Relation to their Technical Applications* (New York: Wiley)